Proceedings of the
American Control Conference
Baltimore, Maryland • June 1994

TM11 - 2:30

Energy Flow Control of Interconnected Structures

Yasuo Kishimoto
Department of Aerospace Engineering
The University of Michigan
Ann Arbor, MI 48109-2118

Dennis S. Bernstein
Department of Aerospace Engineering
The University of Michigan
Ann Arbor, MI 48109-2118

Steven R. Hall
Department of Aeronautics and Astronautics
Massachusetts Institute of Technology
Cambridge, MA 02139

1. Introduction

In [1] active energy flow control techniques were considered for interconnected modal subsystems. These techniques are now applied to interconnected structural subsystems. For this purpose we extend results given in [2] and derive two energy flow models for structures interconnected either conservatively or dissipatively. In the modal subsystem model considered in [1], each mode is viewed as a subsystem, while in the structural subsystem model each substructure is treated as a subsystem. For the modal subsystem model we can directly apply the control techniques considered in [1]. The structural subsystem model, however, requires special care. In particular, a dissipation filter and a disturbance filter are required since now the real part of the substructure impedance and the disturbance spectral density are frequency-dependent.

Two distinct energy flow control techniques developed in [1] are applied to the modal subsystem model and the structural subsystem model. Specifically, the controller is designed either as an additional subsystem or as a dissipative coupling to minimize energy flow entering a specified substructure. The goal in [1] was to maximize the energy flow from a specified subsystem in the modal subsystem model and thus reduce the vibration of this substructure.

In previous works [3,4] H_2 and H_∞ control techniques were used to regulate energy flow in a certain frequency band. In this paper, as in [1], controllers are designed according to a specialized LQG positive real control approach [5] that yields positive real controllers. Thus the resulting controller minimizes an H_2 performance index and guarantees asymptotic stability of the closed-loop system in spite of modeling uncertainty.

2. Structural Model

We consider r one- or two-dimensional structures under vibration by means of pointwise external disturbance forces. Each pair of structures is assumed to be mutually interconnected by means of conservative or dissipative couplings. For convenience, we make the simplifying assumption that all couplings to a given structure are connected to a single point on that structure. The case of structures interconnected at multiple points is more complicated and is outside the scope of this paper.

The partial differential equation for the response of the ith structure is given by

$$\rho_i(\xi)\frac{\partial^2\chi_i(\xi,t)}{\partial t^2} + \mathcal{L}_i\chi_i(\xi,t) = \tilde{w}_i(t)\delta(\xi-\hat{\xi}_i) - h_i(\xi,\xi_{ci},t), \quad (1)$$

where $\xi \in \Omega_i$ denotes the spatial coordinate defined in the region of space Ω_i for the ith structure. Furthermore, $\rho_i(\xi)$ is the mass density, $\mathcal{L}_i$ is the self-adjoint stiffness operator for the ith structure, and $\tilde{w}_i(t)$ is the external disturbance force acting on the ith structure at the point $\hat{\xi}_i$. We assume that $\tilde{w}_i(t)$, $i = 1,\ldots,r$, are mutually uncorrelated white noise disturbances with unit intensity. Additionally, the coupling effect $h_i(\xi,\xi_{ci},t)$ at the coupling position ξ_{ci} is given by

$$h_i(\xi,\xi_{ci},t) \triangleq f_i(t)\delta(\xi-\xi_{ci}), \quad (2)$$

for an interaction force $f_i(t)$.

We consider a modal decomposition of the ith structure of the form

$$\chi_i(\xi,t) = \sum_{j=1}^{\infty} q_{ij}(t)\psi_{ij}(\xi), \quad i = 1,\ldots,r, \quad (3)$$

where $q_{ij}(t)$ and $\psi_{ij}(\xi)$ denote modal coordinates and normalized eigenfunctions, respectively, and the double subscript ij denotes the jth mode of the ith substructure. The normalized eigenfunctions $\psi_{ij}(\xi)$ satisfy the orthogonality properties

$$\int_{\Omega_i}\rho_i(\xi)\psi_{ij}(\xi)\psi_{ik}d\xi = \delta_{jk}, \quad \int_{\Omega_i}\mathcal{L}_i\psi_{ij}(\xi)\psi_{ik}d\xi = \omega_{ij}^2\delta_{jk}, \quad (4)$$

where ω_{ij} is the natural frequency of the jth mode of the ith structure and δ_{jk} is the Kronecker delta. From (3), (4) and appropriate boundary conditions, it follows that the modal coordinates $q_{ij}(t)$ satisfy the equations of motion

$$\ddot{q}_{ij}(t) + 2\zeta_{ij}\omega_{ij}\dot{q}_{ij}(t) + \omega_{ij}^2 q_{ij}(t) = a_{ij}\tilde{w}_i(t) - b_{ij}v_i(t), \quad (5)$$

where $v_i(t)$ is the coupling interaction and the modal damping term $2\zeta_{ij}\omega_{ij}\dot{q}_{ij}(t)$ is now included. In (5), the modal coefficient a_{ij} is defined by

$$a_{ij} \triangleq \psi_{ij}(\hat{\xi}_i), \quad (6)$$

while

$$b_{ij} \triangleq \psi_{ij}(\xi_{ci}), \quad v_i(t) \triangleq f_i(t), \quad (7)$$

for force interaction and

$$b_{ij} \triangleq \frac{\partial\psi_{ij}(\xi_{ci})}{\partial\xi}, \quad v_i(t) \triangleq g_i(t), \quad (8)$$

for torque interaction.

The modal velocity $y_{ij}(t)$ of the jth mode of the ith structure and the velocity $y_i(t)$ of the ith substructure at the coupling point are given by

$$y_{ij}(t) = b_{ij}\dot{q}_{ij}(t), \quad (9)$$

$$y_i(t) = \sum_{j=1}^{n_i} y_{ij}(t), \quad (10)$$

where n_i is the number of modes of the ith structure in the frequency range of interest. For later use we note that the modal impedance $z_{ij}(s)$, $i = 1,\ldots,r$, $j = 1,\ldots,n_i$, is given by

$$z_{ij}(s) = \frac{s^2 + 2\zeta_{ij}\omega_{ij}s + \omega_{ij}^2}{s}. \quad (11)$$

3. Energy Flow Modeling: Modal Subsystem Model

First we obtain the modal subsystem model by considering each mode as a subsystem. Let $w_{ij}(t)$ denote the disturbance force exciting the jth mode of the ith structure, that is,

$$w_{ij}(t) = a_{ij}\tilde{w}_i(t), \quad i = 1,\ldots,r, \; j = 1,\ldots,n_i, \quad (12)$$

and we assume that the coupling interaction $v_i(t)$ and the structural velocity $y_i(t)$ are related by a coupling transfer function $L(s)$, that is,

$$v_s = L(s)y_s, \quad (13)$$

[0]This research was supported in part by the Air Force Office of Scientific Research under Grant F49620-92-J-0127 and the NASA SERC Grant NAGW-1335.

where $y_s(t) \triangleq [y_1(t) \cdots y_r(t)]^T$ and $v_s(t) \triangleq [v_1(t) \cdots v_r(t)]^T$.

To obtain a feedback representation of the interconnected systems, we define the modal impedance matrix

$$Z_m(s) \triangleq \mathrm{diag}(z_{11}(s), z_{12}(s), \ldots, z_{1n_1}(s), \ldots, z_{r1}(s), \ldots, z_{rn_r}(s)), \tag{14}$$

and the vectors

$$y_m(t) \triangleq [\dot{q}_{11}(t) \cdots \dot{q}_{1n_1}(t) \ \dot{q}_{21}(t) \cdots \dot{q}_{2n_2}(t) \ \cdots \ \dot{q}_{r1}(t) \cdots \dot{q}_{rn_r}(t)]^T, \tag{15}$$

$$w_m(t) \triangleq [w_{11}(t) \cdots w_{1n_1}(t) \ w_{21}(t) \cdots w_{2n_2}(t) \ \cdots \ w_{r1}(t) \cdots w_{rn_r}(t)]^T, \tag{16}$$

$$\tilde{w}(t) \triangleq [\tilde{w}_1(t) \ \cdots \ \tilde{w}_r(t)]^T. \tag{17}$$

Note that $w_m(t) = D_m \tilde{w}(t)$, $y_s(t) = E_m^T y_m(t)$ and $v_m(t) = E_m v_s(t)$, where the matrices D_m and E_m are defined by

$$D_m \triangleq \begin{bmatrix} a_{11} & \cdots & a_{1n_1} & 0 & \cdots & 0 & \cdots & 0 & \cdots & 0 \\ 0 & \cdots & 0 & a_{21} & \cdots & a_{2n_2} & & 0 & \cdots & 0 \\ \vdots & \vdots & \vdots & \vdots & \vdots & \vdots & \ddots & \vdots & \vdots & \vdots \\ 0 & \cdots & 0 & 0 & \cdots & 0 & & a_{r1} & \cdots & a_{rn_r} \end{bmatrix}^T, \tag{18}$$

$$E_m \triangleq \begin{bmatrix} b_{11} & \cdots & b_{1n_1} & 0 & \cdots & 0 & \cdots & 0 & \cdots & 0 \\ 0 & \cdots & 0 & b_{21} & \cdots & b_{2n_2} & & 0 & \cdots & 0 \\ \vdots & \vdots & \vdots & \vdots & \vdots & \vdots & \ddots & \vdots & \vdots & \vdots \\ 0 & \cdots & 0 & 0 & \cdots & 0 & & b_{r1} & \cdots & b_{rn_r} \end{bmatrix}^T. \tag{19}$$

With this notation the interconnected system (5) can be expressed as the feedback system shown in Fig. 3.1, where $u_m(t) \triangleq w_m(t) - v_m(t)$ and the coupling matrix $L_m(s)$ for the modal subsystem model satisfying $v_m = L_m y_m$ is defined by

$$L_m(s) \triangleq E_m L(s) E_m^T. \tag{20}$$

Note that if $L(s)$ is conservative, that is, $L(\jmath\omega) + L^*(\jmath\omega) = 0$, it follows that $L_m(\jmath\omega) + L_m^*(\jmath\omega) = 0$ so that $L_m(s)$ is also conservative. In the same manner if $L(s)$ is dissipative, that is, $L(\jmath\omega) + L^*(\jmath\omega) \geq 0$, then $L_m(s)$ is also dissipative, $L_m(\jmath\omega) + L_m^*(\jmath\omega) \geq 0$. Since now $Z_m(s)$ is strictly positive real, the feedback system in Fig. 3.1 is asymptotically stable.

Now we consider three steady-state average energy flows P_{ij}^c, P_{ij}^d and P_{ij}^e, $i = 1, \ldots, r$, $j = 1, \ldots, n_i$ which symbolize

$P_{ij}^c =$ the steady-state average energy flow entering the jth mode of ith structure through the coupling $L_m(s)$,

$P_{ij}^d =$ the steady-state average energy dissipation rate of the jth mode of ith structure,

$P_{ij}^e =$ the steady-state average external power entering the jth mode of ith structure.

To evaluate these steady-state average energy flows consider state-space realizations of $Z_m^{-1}(s)$ and $L(s)$ in Fig. 3.1 given by

$$\dot{x}_m(t) = A_m x_m(t) + B_m u_m(t), \tag{21}$$

$$y_m(t) = C_m x_m(t), \tag{22}$$

$$\dot{x}_L(t) = A_L(t) x_L(t) + B_L y_s(t), \tag{23}$$

$$v_s(t) = C_L x_L(t), \tag{24}$$

respectively. Since $u_m(t) = w_m(t) - v_m(t) = D_m \tilde{w}(t) - E_m v_s(t)$ and $y_s(t) = E_m^T y_m(t)$, the augmented system (21)-(24) is given by

$$\dot{x}_{am}(t) = \tilde{A} x_{am}(t) + \tilde{D} \tilde{w}(t), \tag{25}$$

where $x_{am}(t) \triangleq \begin{bmatrix} x_m(t) \\ x_L(t) \end{bmatrix}$,

$$\tilde{A} \triangleq \begin{bmatrix} A_m & -B_m E_m C_L \\ B_L E_m^T C_m & A_L \end{bmatrix}, \ \tilde{D} \triangleq \begin{bmatrix} B_m D_m \\ 0 \end{bmatrix}.$$

Also define C_{m1} and C_{m2} by

$$C_{m1} \triangleq [C_m \quad 0], \quad C_{m2} \triangleq [0 \quad E_m C_L], \tag{26}$$

so that $y_m(t) = C_{m1} x_{am}(t)$ and $v_m(t) = C_{m2} x_{am}(t)$.

Next we define the diagonal damping matrix

$$C_{md} \triangleq \mathrm{Re}[Z_m(s)], \tag{27}$$

and note that (11) and (14) imply

$$C_{md\,ijij} = 2\zeta_{ij}\omega_{ij}, \tag{28}$$

where A_{ijpq} denotes $A_{(n_{ij}, n_{pq})}$ and $n_{ij} \triangleq (\sum_{l=1}^{i-1} n_l) + j$. With this notation the steady-state average energy flows P_{ij}^c, P_{ij}^d and P_{ij}^e are given by [2]

$$P_{ij}^c = -\mathcal{E}[\dot{q}_{ij} v_{m(n_{ij})}] = -(C_{m2} \tilde{Q}_m C_{m1}^T)_{ijij}, \tag{29}$$

$$P_{ij}^d = -\mathcal{E}[\dot{q}_{ij} u_{m(n_{ij})}] = -(C_{md} C_{m1} \tilde{Q}_m C_{m1}^T)_{ijij}, \tag{30}$$

$$P_{ij}^e = \mathcal{E}[\dot{q}_{ij} w_{m(n_{ij})}] = \frac{1}{2}(D_m \tilde{D}^T C_{m1}^T)_{ijij}, \tag{31}$$

where $v_{m(n_{ij})}$, $u_{m(n_{ij})}$ and $w_{m(n_{ij})}$ are the n_{ij}th element of $v_m(t)$, $u_m(t)$ and $w_m(t)$, respectively, and the steady-state covariance $\tilde{Q}_m \triangleq \lim_{t\to\infty} \mathcal{E}[x_{am}(t) x_{am}^T(t)]$ satisfies the algebraic Lyapunov equation

$$\tilde{A}\tilde{Q}_m + \tilde{Q}_m \tilde{A}^T + \tilde{D}\tilde{D}^T = 0. \tag{32}$$

As shown in [2], P_{ij}^c, P_{ij}^d and P_{ij}^e satisfy

$$P_{ij}^c + P_{ij}^d + P_{ij}^e = 0, \ i = 1, \ldots, r, \ j = 1, \ldots, n_i. \tag{33}$$

Furthermore, if $L(s)$ is conservative, then [2]

$$\sum_{i=1}^{r} \sum_{j=1}^{n_i} P_{ij}^c = 0, \tag{34}$$

while if $L(s)$ is dissipative, then [2]

$$\sum_{i=1}^{r} \sum_{j=1}^{n_i} P_{ij}^c \leq 0. \tag{35}$$

4. Energy Flow Modeling: Structural Subsystem Model

Now we obtain the structural subsystem energy flow model by treating each substructure as a subsystem. In this model the energy flows are evaluated at the coupling points of the substructures. Hence the total impedance $z_i(s)$ of the ith structure at the coupling point is given by

$$\frac{1}{z_i(s)} = \sum_{j=1}^{n_i} \frac{b_{ij}^2}{z_{ij}(s)}, \tag{36}$$

for $i = 1, \ldots, r$. Additionally, by using the fact that the transfer admittance from the external force $\tilde{w}_i(t)$ at $\hat{\xi}_i$ to the velocity $y_i(t)$ at ξ_{c_i} is given by $\sum_{j=1}^{n_i} \frac{a_{ij} b_{ij}}{z_{ij}(s)}$, it follows that the filter function $T_i(s)$ defined by

$$T_i(s) \triangleq z_i(s) \sum_{j=1}^{n_i} \frac{a_{ij} b_{ij}}{z_{ij}(s)} \tag{37}$$

transforms the external disturbance force $\tilde{w}_i$ at $\hat{\xi}_i$ into the disturbance force w_i at the coupling point ξ_{c_i}, that is,

$$w_i = T_i \tilde{w}_i. \tag{38}$$

With this notation (5) can be rewritten as

$$z_i(s) y_i = w_i - v_i. \tag{39}$$

Since $z_i(s)$ is strictly positive real, it follows that

$$c_i(\omega) \triangleq \mathrm{Re}[z_i(\jmath\omega)] > 0, \quad i = 1, \ldots, r, \quad \omega \in \mathcal{R}, \tag{40}$$

where $c_i(\omega)$ is the frequency-dependent resistance or damping. For convenience, define the $r \times r$ diagonal transfer function

$$Z_s(s) \triangleq \mathrm{diag}(z_1(s), \ldots, z_r(s)), \tag{41}$$

and the frequency-dependent resistance or damping matrix

$$C_d(\jmath\omega) \triangleq \mathrm{Re}[Z_s(\jmath\omega)] = \mathrm{diag}(c_1(\omega), \ldots, c_r(\omega)). \tag{42}$$

With this notation the interconnected system in (39) can be expressed as a feedback system in Fig. 4.1. In Fig. 4.1 $w_s(t) \triangleq [w_1(t) \cdots w_r(t)]^{\mathrm{T}}$, $u_s(t) \triangleq [u_1(t) \cdots u_r(t)]^{\mathrm{T}} = w_s(t) - v_s(t)$ and $y_s(t)$, $v_s(t)$ and $L(s)$ satisfy (13).

Now we consider the steady-state average energy flow among substructures. In a similar manner to the previous section the steady-state average energy flows P_i^c, P_i^d and P_i^e are defined for $i = 1, \ldots, r$ by

$$P_i^c \triangleq -\mathcal{E}[y_i(t)v_i(t)], \tag{43}$$

$$P_i^d \triangleq -\mathcal{E}[y_i(t)u_i(t)], \tag{44}$$

$$P_i^e \triangleq \mathcal{E}[y_i(t)w_i(t)], \tag{45}$$

where $u_i(t)$ is the ith element of $u_s(t)$. The meaning of these energy flow quantities corresponds to the meanings of P_{ij}^c, P_{ij}^d and P_{ij}^e in the previous section, respectively, but now P_i^c, P_i^d and P_i^e are the energy flows for the ith substructure and P_i^c is the energy flow through the coupling $L(s)$ in Fig. 4.1.

In the previous section we expressed $P_{ij}^c, P_{ij}^d, P_{ij}^e$ in terms of the steady-state covariance $\tilde{Q}_m$ according to the approach in [2,3]. In the structural energy flow model, however, the real part $c_i(s)$ of $z_i(s)$, is not constant and the disturbance $w_i(t)$ entering $z_i(s)$ is no longer white noise. Thus to obtain the steady-state covariance corresponding to $\tilde{Q}_m$ we now introduce two filter transfer function matrices $T(s)$ and $R_d(s)$ as shown in Fig. 4.1, where the disturbance filter $T(s)$ is defined by

$$T(s) \triangleq \mathrm{diag}(T_1(s), T_2(s), \ldots, T_r(s)), \tag{46}$$

and the stable dissipation filter $R_d(s)$ satisfying [4]

$$R_d(s)R_d^{\mathrm{T}}(-s) = C_d(s). \tag{47}$$

Now let $Z_s^{-1}(s)$, $T(s)$ and $R_d(s)$ have the realizations

$$\dot{x}_s(t) = A_s x_s(t) + B_s u_s(t), \tag{48}$$

$$y_s(t) = C_s x_s(t), \tag{49}$$

$$\dot{x}_w(t) = A_w x_w(t) + B_w \tilde{w}(t), \tag{50}$$

$$w_s(t) = C_w x_w(t) + D_w \tilde{w}(t), \tag{51}$$

$$\dot{x}_R(t) = A_R x_R(t) + B_R y_s(t), \tag{52}$$

$$y_R(t) = C_R x_R(t) + D_R y_s(t), \tag{53}$$

respectively. By considering the state space model of $L(s)$ given in (23) and (24) the augmented system is given by

$$\dot{x}_{as}(t) = \tilde{A} x_{as}(t) + \tilde{D}\tilde{w}(t), \tag{54}$$

where $x_{as}(t) \triangleq [\ x_s(t) \quad x_w(t) \quad x_R(t) \quad x_L(t)\ ]^{\mathrm{T}}$, and

$$\tilde{A} \triangleq \begin{bmatrix} A_s & B_s C_w & 0 & -B_s C_L \\ 0 & A_w & 0 & 0 \\ B_R C_s & 0 & A_R & 0 \\ B_L C_s & 0 & 0 & A_L \end{bmatrix}, \quad \tilde{D} \triangleq \begin{bmatrix} B_s D_w \\ B_w \\ 0 \\ 0 \end{bmatrix}.$$

Furthermore, define

$$C_{s1} \triangleq [C_s \ \ 0 \ \ 0 \ \ 0], \quad C_{s2} \triangleq [0 \ \ 0 \ \ 0 \ \ C_L], \quad C_{sd} \triangleq [D_R C_s \ \ 0 \ \ C_R \ \ 0],$$

so that $y_s(t) = C_{s1}x_{as}(t)$, $v(t) = C_{s2}x_{as}(t)$ and $y_R(t) = C_{sd}x_{as}(t)$.

With the above notation, P_i^c and P_i^d are given by [2]

$$P_i^c = -(C_{s2}\tilde{Q}_s C_{s1}^{\mathrm{T}})_{(i,i)}, \tag{55}$$

$$P_i^d = -(C_{sd}\tilde{Q}_s C_{sd}^{\mathrm{T}})_{(i,i)}, \tag{56}$$

where the steady-state covariance $\tilde{Q}_s \triangleq \lim_{t\to\infty} \mathcal{E}[x_{as}(t)x_{as}^{\mathrm{T}}(t)]$ satisfies

$$0 = \tilde{A}\tilde{Q}_s + \tilde{Q}_s\tilde{A}^{\mathrm{T}} + \tilde{D}\tilde{D}^{\mathrm{T}}. \tag{57}$$

As in the modal subsystem energy flow model, P_i^c, P_i^d and P_i^e satisfy

$$P_i^c + P_i^d + P_i^e = 0, \tag{58}$$

Furthermore if $L(s)$ is conservative, then

$$\sum_{i=1}^{r} P_i^c = 0, \tag{59}$$

while if $L(s)$ is dissipative, then

$$\sum_{i=1}^{r} P_i^c \leq 0. \tag{60}$$

5. Design of an Energy Flow Controller as an Additional Subsystem: Modal Subsystem Model

In this section we consider a control problem involving $r-1$ structures interconnected by a stiffness (lossless) coupling and design the controller as an additional subsystem.

Now we connect the single-input single-output controller $z_c^{-1}(s)$ to the structures $Z_m^{-1}(s)$ whose state space model is given by (21) and (22). The additional subsystem, that is, the controller $z_c^{-1}(s)$ is assumed to be expressed by

$$\dot{x}_c(t) = A_c x_c(t) + B_c y(t), \tag{61}$$

$$u(t) = C_c x_c(t), \tag{62}$$

where $u(t)$ and $y(t)$ are scalars and we now assume that the disturbance does not directly enter into the controller $z_c^{-1}(s)$. Then the augmented feedback representation of the feedback system corresponding to Fig. 3.1 is shown in Fig. 5.1. In Fig. 5.1

$$E_a \triangleq \begin{bmatrix} E_m & 0 \\ 0 & 1 \end{bmatrix}, \quad D_a \triangleq \begin{bmatrix} D_m \\ 0 \end{bmatrix},$$

where D_m and E_m are defined by (18), (19), respectively.

As shown in Fig. 5.1 the admittance matrix corresponding to $Z_m^{-1}(s)$ in Fig. 3.1 is now comprised of $Z_m^{-1}(s)$ and $z_c^{-1}(s)$. In this case the augumented vectors $y_{am}(t)$, $u_{am}(t)$, $w_{am}(t)$ and $w_a(t)$ in Fig. 5.1 are defined by

$$y_{am}(t) \triangleq \begin{bmatrix} y_m(t) \\ u(t) \end{bmatrix}, \quad u_{am}(t) \triangleq \begin{bmatrix} u_m(t) \\ y(t) \end{bmatrix},$$

$$w_{am}(t) \triangleq \begin{bmatrix} w_m(t) \\ 0 \end{bmatrix}, \quad w_a(t) \triangleq \begin{bmatrix} \tilde{w}(t) \\ 0 \end{bmatrix},$$

respectively.

On the other hand the stiffness coupling $L(s)$ is now expressed by

$$L(s) = \frac{1}{s}C_L, \tag{63}$$

where the symmetric matrix $C_L \in \mathcal{R}^{r\times r}$ is partitioned as

$$C_L \triangleq \begin{bmatrix} C_{L_{11}} & C_{L_{12}} \\ C_{L_{12}}^{\mathrm{T}} & C_{L_{22}} \end{bmatrix}. \tag{64}$$

We define the position vectors $y_{\mathrm{pm}}(t) \triangleq \int y_{\mathrm{m}}(t)dt = C_{\mathrm{pm}}x_{\mathrm{m}}(t)$ for $Z_{\mathrm{m}}^{-1}(s)$ and a scalar state $x_{\mathrm{pc}}(t)$ by

$$\dot{x}_{\mathrm{pc}}(t) \triangleq u(t), \tag{65}$$

for the controller $z_{\mathrm{c}}^{-1}(s)$ so that the output vector v_{am} of the stiffness coupling $L_{\mathrm{m}}(s)$ is given by

$$v_{\mathrm{am}} = E_{\mathrm{a}}\frac{1}{s}C_L E_{\mathrm{a}}^{\mathrm{T}} y_{\mathrm{am}} = E_{\mathrm{a}} C_L \begin{bmatrix} C_{\mathrm{pm}} E_{\mathrm{m}}^{\mathrm{T}} x_m \\ x_{\mathrm{pc}} \end{bmatrix}. \tag{66}$$

By using (61) - (66) the feedback system shown in Fig. 5.1 is expressed as

$$\dot{x}_{\mathrm{am}}(t) = \tilde{A}x_{\mathrm{am}}(t) + \tilde{D}\tilde{w}(t), \tag{67}$$

where

$$\tilde{A} \triangleq \begin{bmatrix} A_{\mathrm{m}} - B_{\mathrm{m}}E_{\mathrm{m}}C_{L_{11}}E_{\mathrm{m}}^{\mathrm{T}}C_{\mathrm{pm}} & -B_{\mathrm{m}}E_{\mathrm{m}}C_{L_{12}} & 0 \\ 0 & 0 & C_{\mathrm{c}} \\ -B_{\mathrm{c}}C_{L_{12}}^{\mathrm{T}}E_{\mathrm{m}}^{\mathrm{T}}C_{\mathrm{pm}} & -B_{\mathrm{c}}C_{L_{22}} & A_{\mathrm{c}} \end{bmatrix},$$

$$\tilde{D} \triangleq \begin{bmatrix} B_{\mathrm{m}}D_{\mathrm{m}} \\ 0 \\ 0 \end{bmatrix}, \quad x_{\mathrm{am}}(t) \triangleq \begin{bmatrix} x_{\mathrm{m}}(t) \\ x_{\mathrm{pc}}(t) \\ x_{\mathrm{c}}(t) \end{bmatrix}.$$

Furthermore, define

$$C_{\mathrm{am}} \triangleq [C_{\mathrm{m}} \quad 0 \quad 0], \tag{68}$$

so that $y_{\mathrm{am}}(t) = C_{\mathrm{am}}x_{\mathrm{am}}(t)$.

We now determine $(A_{\mathrm{c}}, B_{\mathrm{c}}, C_{\mathrm{c}})$ by means of the LQG positive real approach. By defining $x(t) \triangleq \begin{bmatrix} x_{\mathrm{m}}(t) \\ x_{\mathrm{pc}}(t) \end{bmatrix}$, and

$$A \triangleq \begin{bmatrix} A_{\mathrm{m}} - B_{\mathrm{m}}E_{\mathrm{m}}C_{L11}E_{\mathrm{m}}^{\mathrm{T}}C_{\mathrm{pm}} & -B_{\mathrm{m}}E_{\mathrm{m}}C_{L12} \\ 0 & 0 \end{bmatrix}, \ B \triangleq [0 \cdots 0 \ 1]^{\mathrm{T}},$$

$$C \triangleq [-C_{L21}E_{\mathrm{m}}^{\mathrm{T}}C_{\mathrm{pm}} \quad -C_{L22}], \quad D_1 \triangleq \begin{bmatrix} B_{\mathrm{m}}D_{\mathrm{m}} \\ 0 \end{bmatrix},$$

it follows that $\tilde{A}$ and $\tilde{D}$ in (67) can be expressed as

$$\tilde{A} = \begin{bmatrix} A & BC_{\mathrm{c}} \\ B_{\mathrm{c}}C & A_{\mathrm{c}} \end{bmatrix}, \quad \tilde{D} = \begin{bmatrix} D_1 \\ B_{\mathrm{c}}D_2 \end{bmatrix}, \tag{69}$$

where D_2 in $\tilde{D}$ represents fictitious measurement noise required by the LQG approach.

Now the controller is required to reduce the vibration of a specified substructure. For this purpose we define the total energy flow through the coupling to all n_i modes of the ith structure $\mathcal{P}_i^{\mathrm{c}}$ given by $\mathcal{P}_i^{\mathrm{c}} = \sum_{j=1}^{n_i} P_{ij}^{\mathrm{c}}$, while $\mathcal{P}_i^{\mathrm{d}}$ and $\mathcal{P}_i^{\mathrm{e}}$ defined by

$$\mathcal{P}_i^{\mathrm{d}} \triangleq \sum_{j=1}^{n_i} P_{ij}^{\mathrm{d}}, \qquad \mathcal{P}_i^{\mathrm{e}} \triangleq \sum_{j=1}^{n_i} P_{ij}^{\mathrm{e}}$$

have a similar interpretation. Furthermore, from (33) it follows that

$$\mathcal{P}_i^{\mathrm{c}} + \mathcal{P}_i^{\mathrm{e}} = -\mathcal{P}_i^{\mathrm{d}}. \tag{70}$$

Since $\mathcal{P}_i^{\mathrm{c}}$ represents energy flow entering the ith structure through the coupling and $\mathcal{P}_i^{\mathrm{e}}$ represents external energy flow entering the ith structure, it follows that the left hand side of (70) represents the total energy flow entering the ith structure. Hence by minimizing $-\mathcal{P}_i^{\mathrm{d}}$, we can minimize the total energy flow entering the ith structure and as a result we can reduce the vibration of the ith structure.

Now defining the augmented diagonal matrix C_{am}

$$C_{\mathrm{am}} \triangleq \begin{bmatrix} C_{\mathrm{md}} & 0 \\ 0 & 0 \end{bmatrix}, \tag{71}$$

where C_{md} is defined (27), and using (70) with (30) and (67) yields

$$-\mathcal{P}_i^{\mathrm{d}} = \mathcal{E}[x_{\mathrm{am}}^{\mathrm{T}}C_{\mathrm{am}}^{\mathrm{T}}\tilde{C}_1C_{\mathrm{am}}x_{\mathrm{am}}],$$

where the steady-state covariance $\tilde{Q}_{\mathrm{am}} \triangleq \lim_{t\to\infty}\mathcal{E}[x_{\mathrm{am}}(t)x_{\mathrm{am}}^{\mathrm{T}}(t)]$ satisfies

$$0 = \tilde{A}\tilde{Q}_{\mathrm{am}} + \tilde{Q}_{\mathrm{am}}\tilde{A}^{\mathrm{T}} + \tilde{D}\tilde{D}^{\mathrm{T}}, \tag{72}$$

and

$$\tilde{C}_1 \triangleq \sum_{j=1}^{n_i} e_{n_{ij}}e_{n_{ij}}^{\mathrm{T}}C_{\mathrm{am}}. \tag{73}$$

Thus letting the performance variables have the form

$$z(t) = E_1x(t) + E_2u(t), \tag{74}$$

it follows that E_1 is given by $E_1 = \tilde{C}_1^{1/2}C_{\mathrm{am}}$.

6. Example

We design an energy flow controller to serve as a dissipative coupling for two uniform cantilever beams as shown in Fig. 6.1. The beams are of lengths L_1, L_2, mass densities ρ_1, ρ_2, and bending stiffnesses E_1I_{A1}, E_2I_{A2}, respectively. Each beam is subjected to mutually uncorrelated white noise disturbances $\tilde{w}_i(t), i = 1, 2$, with unit intensity applied at $\hat{\xi}_i$ and with control force from the coupling controller $f_{\mathrm{c}}(t)$ applied at ξ_{ci}.

We consider the first three modes of each beam and let $L_1 = 3, L_2 = 2.5$, $\rho_1 = \rho_2 = 1$, $E_1L_{A1} = 1$, $E_2I_{A2} = 1.1^2$, $\zeta_{1j} = 0.01, \zeta_{2j} = 0.02$, $j = 1, 2, 3$, $\hat{\xi}_1 = 1, \hat{\xi}_2 = 1.5$ and $\xi_{c1} = \xi_{c2} = 2.2$.

To reduce the vibration of the ith beam, $i = 1, 2$, we design four controllers. Controllers 1 and 2 are designed by the modal subsystem model to minimize $-\mathcal{P}_1^{\mathrm{d}}$ and $-\mathcal{P}_2^{\mathrm{d}}$, respectively, while Controllers 3 and 4 are designed by the structural subsystem model to minimize $-P_1^{\mathrm{d}}$ and $-P_2^{\mathrm{d}}$, respectively. The resulting energy flow diagrams are illustrated in Figs. 6.2 and 6.3 for the modal subsystem model and the structural subsystem model, respectively, where OL denotes the open-loop system and G_{ci} represents Controller i. Figs. 6.2 and 6.3 show that the controller absorbs energy from all of the subsystems and minimizes the energy dissipation from each beam. Furthermore, Controllers 1 and 2 remove maximal energy from beams 1 and 2, respectively, while Controllers 3 and 4 minimize the total energy flow entering beams 1 and 2, respectively.

[1] Kishimoto, Y., Bernstein, D. S., and Hall, S. R., "Dissipative Control of Energy Flow in Interconnected Systems," *Proc. AIAA GNC Conf.*, 1993 Monterey, CA, pp. 657-666.

[2] Kishimoto, Y., and Bernstein, D. S., "Thermodynamic Modeling of Interconnected Systems: I. Conservative Coupling, II. Dissipative Coupling," to appear in *J. Sound Vib.*

[3] Miller, D. W., Hall, S. R., and von Flotow, A. H., "Optimal Control of Power Flow at Structural Junctions," *J. Sound Vib.*, Vol. 140, No. 3, pp. 475-497, 1990.

[4] MacMartin, D. G., and Hall, S. R., "Control of Uncertain Structures Using an H_∞ Power Flow Approach," *J. Guid. Contr. Dyn.*, Vol. 14, pp. 521-530, 1991.

[5] W. M. Haddad, D. S. Bernstein, and Y. W. Wang, "Dissipative H_2/H_∞ Controller Synthesis," *Proc. Amer. Contr. Conf.*, pp. 243-244, San Francisco, CA, June 1993.

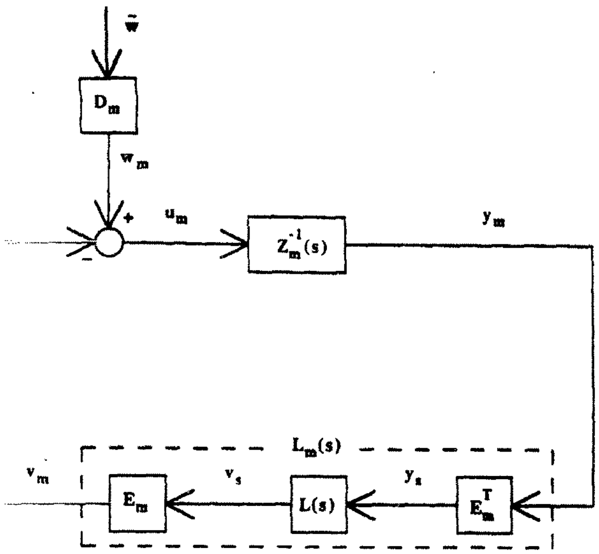

Fig. 3.1. Feedback Representation of Modal Subsystem Model.

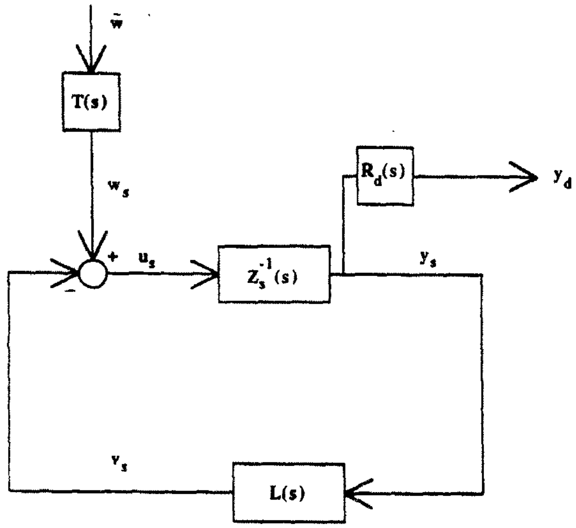

Fig. 4.1. Feedback Representation of Structural Subsystem Model.

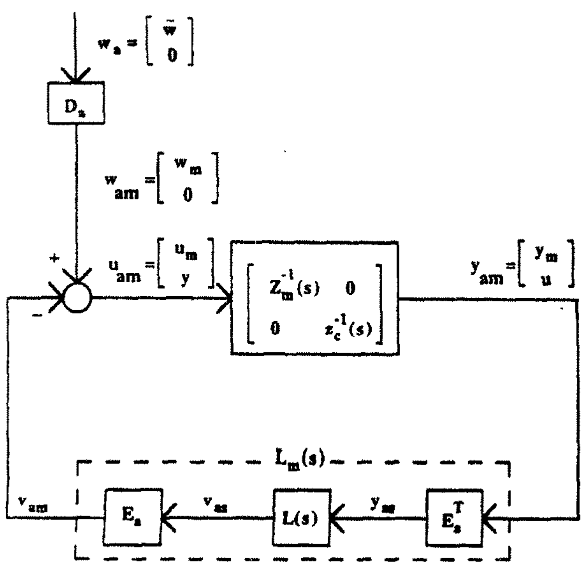

Fig. 5.1. Feedback Representation of Plant and Controller (Modal Subsystem Model).

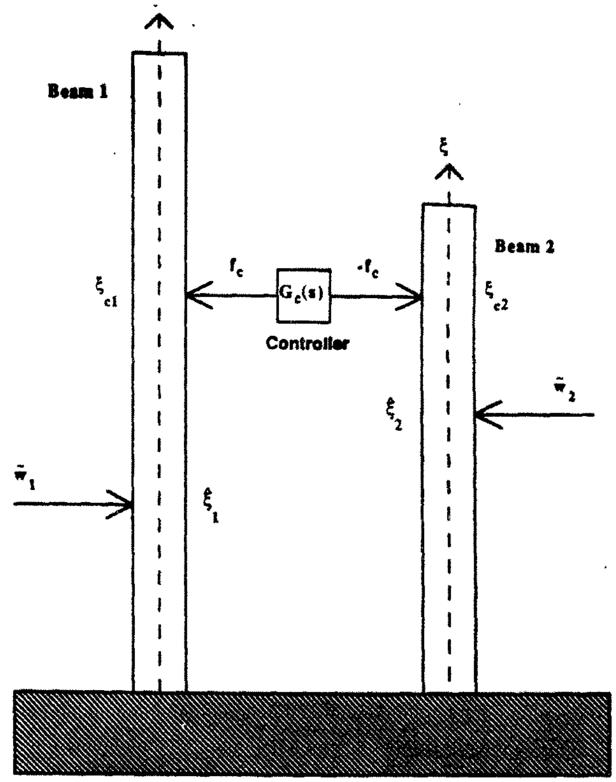

Fig. 6.1 Two Cantilever Beams with Controller Coupling.

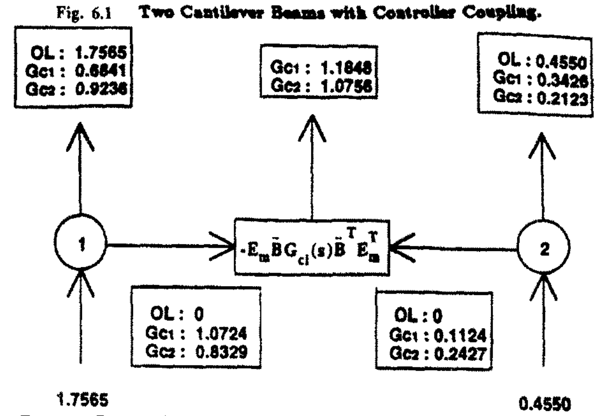

Fig. 6.2. Energy Flow between Beams with Controllers G_{c1} and G_{c2} based on the Modal Subsystem Model.

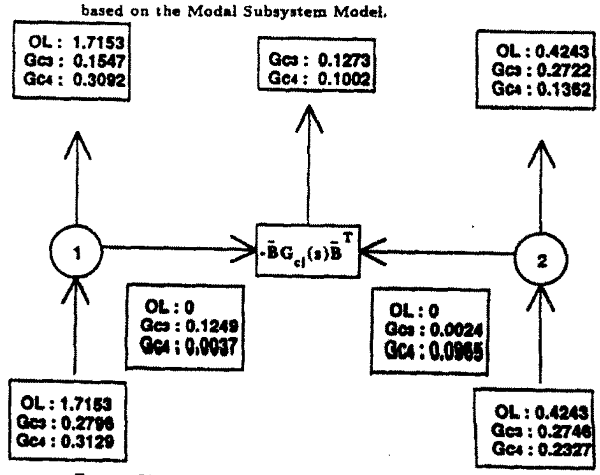

Fig. 6.3. Energy Flow between Beams with Controllers G_{c3} and G_{c4} based on the Structural Subsystem Model.